Int. J. Electrochem. Sci., 14 **(2019)** 9671 – 9681, doi: 10.20964/2019.07.17

International Journal of
ELECTROCHEMICAL
SCIENCE
www.electrochemsci.org

A Mechanistic Study of Corrosion of Graphene and Low zinc-rich Epoxy Coatings on Carbon Steel in Salt Environment

Shengrong Wang[1,2,], Jianwei Yang[1,2], Jianping Cao[1,2], Lijun Gao[1,2],Chenxi Yan[1,2]*

[1] Shougang Research Institute of Technology, Beijing 100043
[2] Beijing key Laboratory of Green Recyclable Process for Iron & steel Production Technology, Beijing 100043)
[*]E-mail: wangshengrong@126.com

Received: 9 February 2019 / *Accepted:* 21 April 2019 / *Published:* 30 August 2019

The effect of graphene on zinc-rich epoxy coating comprised of 40 wt % Zn has been studied.The potential-time measurement, electrochemical impedance spectroscopy (EIS), salt spray fog and UV-aging cyclic aging test and scanning electron microscopy (SEM) were used to characterize the protection performance of coatings. The results show that the zinc-rich epoxy coating reinforced with 2.0 wt% graphene has greatly improved the corrosion protection of coating. Also, the permeability of zinc-rich epoxy coating can be improved by adding adequate amounts of graphene. Graphene nanosheets could enhance the conductivity of zinc particles by introducing the graphene into zinc-rich epoxy coatings and improved the utilization of zinc powders, finally, the life of zinc-rich epoxy coating was prolonged.

Keywords: Zinc-rich epoxy; Graphene sheets; Corrosion protection

1. INTRODUCTION

Application of anticorrosion coatings is one of the most effective and practical methods in metal protection. Since the 1930s, zinc-rich coatings have received extensive attention in different coating systems, and have been widely used in marine and industrial environments. Zinc-rich epoxy coatings have successfully provided good protection for ships, offshore oil platforms, wharfs, gates, tanks, pipelines and bridges[1-4].

There are three protective mechanisms in zinc-rich epoxy coatings [5]: the first mechanism is cathodic protection, a good conductive network is formed between zinc powders and steel substrate which enough zinc powders exist in the coating. As the electrode potential of zinc is much more negative than iron and zinc powders will be preferentially corroded, thus the steel matrix is protected. This is the most characteristic anticorrosive mechanism of zinc-rich coatings. The second mechanism is the physical shielding effect. It is insoluble zinc salts and complexes of zinc corrosion produces, and these stable

compounds deposit on the coating surface which prevent the corrosive medium from penetrating the substrate surface. The third mechanism is the self-healing and passivation of the film.

The standard potential of Zn is -0.762 V vs.SCE, and it is lower than Fe (-0.440 V vs.SCE). A corrosion cell will be formed between the coating and zinc particles when the water penetrates into the coating. In the initial stage, zinc particles preferentially occur anodic reaction and lose electrons, while steel obtain electrons on the cathode to be protected[6], so it is the cathodic protection effect. As the corrosion time extension, corrosion products of zinc filled the pore and defect of the coating, therefore blocking the passage of corrosive particles, which is the primary principle of physical shielding effect of zinc-rich coatings[7]. The steel substrate will be exposed when the coating is destroyed by external force. Corrosion current flows through the exposed areas, where the corrosion products generate a protective layer over a long period of time for the accumulation of production, which is the self-healing effect of the film [8]. The zinc content in the coatings must be more than 80 wt% in order to ensure good electrical contact between zinc fillers and steel substrates. However, the increase of zinc content will reduce the flexibility of the coatings, weaking the adhesion of the steel substrate, also increasing the viscosity of the coatings, then resulting in poor spraying ability and poor leveling properties [9-10]. In the later stage of coating service, zinc corrosion products gradually increased and the electrical contact between the zinc powder and the steel substrate are weakened, also, the cathodic protection of the coatings are weakened gradually. A certain amount of fillers are used to replace some zinc powders, which can make the zinc-rich coating have better corrosion resistance with the low content of zinc. Recently, researchers have been made to use conductive particles as fillers to improve coating conductivity with a lower loading of zinc [11-18]. However, most of these studies has not successful achieved the ultimate goals. Thus, the modification of zinc-rich coatings with proper conductive additives is still a research direction.

In the past decade, graphene (G) has gradually attracted attention of researchers from academic to industry fields for the unique nanostructure, excellent physical properties, large specific surface area, super hydrophobicity and good compatibility with polymer matrix. It is a new type of two-dimensional structure with a single layer thickness approximately 0.335 nm and a diameter ranging from several microns to several hundred microns[19, 20].

It has been reported that graphene displayed excellent corrosion resistance and self-lubricant characteristics. As it has a unique flexible graphite layer, superhydrophobic, good electrical conductivity, extremely high strength and easy shear capability on its densely packed and atomically smooth surface [21-22]. Therefore, well-dispersed graphene can be used in coating to obtain good shielding and conductivity properties, which can make up the relative deficiency of zinc-rich coating.

2. MATERIALS AND METHODS

2.1 Preparation of Coating Samples

The zinc-rich epoxy (ZRE) coating was prepared from a commercially available company of Beijing Hongshi Paint Co., Ltd. The zinc-rich epoxy coating contains 40 wt% zinc particles. The few layered graphene particles were purchased from Tianyuan (Shenzheng) Empire Materials Co., Ltd .

Adding a certain amount of graphene to the zinc-rich epoxy coating according to the weight of the primer. In order to continuous uniformly disperse the graphene into coating, it is necessary to add a certain amount of graphene nanosheets to acetone solution and form a suspension by high-speed disperse machine. Then, the graphene suspension was mixed with zinc-rich epoxy paint and sonicated for 30 min. The mixture was further stirred for 1 h at room temperature. Finally, epoxy resin and a polyamide hardener with the weight ratio of 9:1 was added to the mixture under stiring. Prepared coatings were brushed on carbon steel with a chemical composition (wt%) of C 0.10～0.20%, Si 0.4～0.5%, Mn 1～2%, P 0.01～0.02%, S 0.002～0.003%, Cr 0.01～0.03%, Mo 0.005～0.006%, Fe 98.47～97.25%.

The zinc-rich epoxy paint was sprayed on carbon steel substrates and the dimension of carbon steel substrates of 150×75×3 mm. The steel substrates need to be sandblasted and degreased with acetone, and finally dried at room temperature. Coating systems were kept at room temperature for seven days before the experiment carried out. The dry film thickness was measured by an Elcometer 456 coating thickness gauge. The thickness of coating was 110±10μm.

2.2 Electrochemical Measurements

The electrochemical measurements were carried out by using a PARSTAT 4000 electrochemical workstation. A traditional three-electrode cell was used as a electrochemical measurement system at room temperature. Coating was used as the working electrode, an Ag/AgCl (3M KCl) electrode was used as the reference electrode, and Pt electrode was the counter electrode. The electrochemical tests included open circuit potential (OCP) test and electrochemical impedance spectroscopy (EIS) test. During EIS measurements, the coatings were exposed to a 3.5wt% NaCl solution. Impedance measurements were performed at open circuit potential. Using a 20 mV amplitude of the sinusoidal voltage with a frequency range of 0.1 MHz to 10 mHz.

2.3 Salt Spray and UV-aging Cyclic Aging Test

In order to get the testing conditions close to the nature, the methods of salt spray and UV-aging cycle testing were adopted, including one-week salt spray test (ASTM B117) and one-week QUV accelerated aging test (ASTM D4587), and duration of time 2000h.

2.4. Morphology Characterization

The Microstructures of Graphene were observed by Transmission Electron Microscope (TEM).

Transmission Electron Microscope (TEM) was carried out by using a JEM 2100F (UHR, Japan) and operated in the voltage of 200kV. Scanning electron microscope (SEM S-3400N) was used to observe the surface morphology of coatings before and after Salt Spray and UV-aging Cycle Testing.

3. RESULTS AND DISCUSSION

3.1 Microtopography of graphene

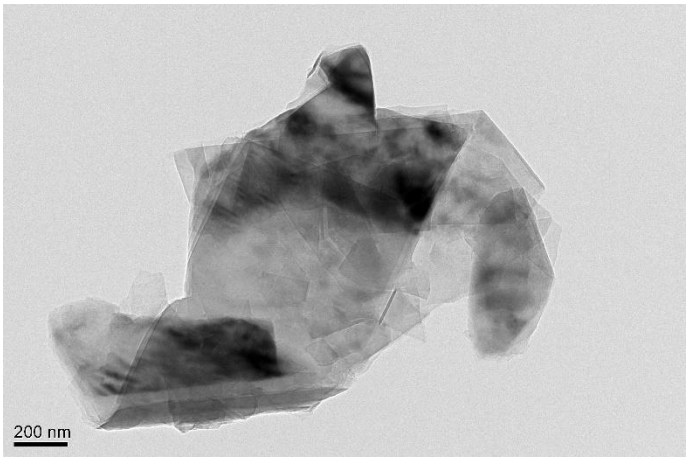

Figure 1. The Transmission Electron Microscope (TEM) image of the graphene particles.

Fig. 1 shows TEM image of the graphene sheet. It is irregular, folding and layer structured neat graphene sheets. However, the layers are entangled and curled with each other, as a result of van der Waals interactions[23]. The graphene sheets are larger than 6.05 μm in width and 11.16μm in length. The crumpled and rippled structure of graphene was found.

3.2 Measurement of open circuit potential (OCP)

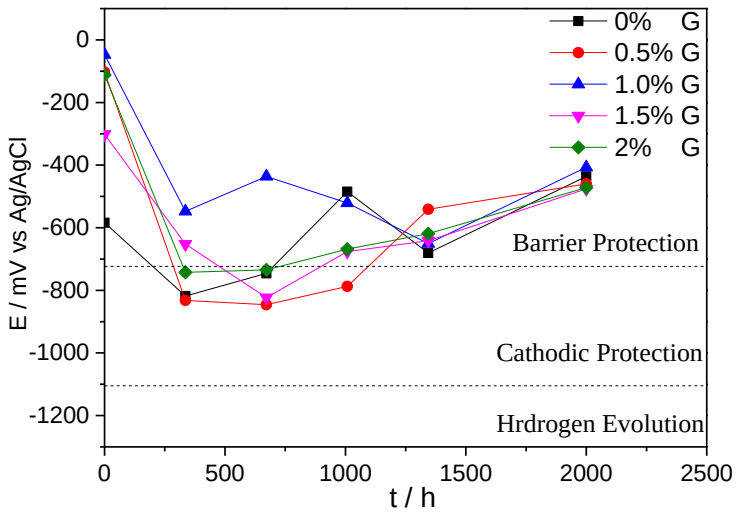

Figure 2. Open circuit potential (OCP) evolution of 40 wt% zinc-rich epoxy coating with different graphene contents worked on cyclic aging experiment as time.

There are maximum and minimum cathodic protection potentials for steel materials. Some researchers indicated that a maximum value of -0.72 V vs Ag / AgCl in 0.5 M KCl solution, which

represented the failure of cathodic protection[24,25]. The zinc-rich epoxy coating worked as a cathodic protection when the system potential was lower than this value, however, cathodic protection of the coating disappeared when the system potential was higher than this value.

Fig.2 shows the change of potential on the surface of coatings with time which worked in cyclic aging experiment during 2000 hours. The critical cathodic protection potential -0.72 V vs. Ag/AgCl/ as the boundary value. Zinc particles can be considered as sacrificial anode particles, it will be preferential corroded to protect the steel substrate from damage while immersed in the electrolyte [26,27]. A more negative open circuit potential meaning zinc particles provide better cathodic protection. As shown in Fig.2, the potential of 0.5% G-ZRE and 1.5% G-ZRE coatings are more negative and can be explained for the percolation effect of graphene nanoparticles which resulted in better electrical contact between zinc particles.

As shown in Fig.2, during 0 hours and 350 hours of the aging time, the open circuit potential declined rapidly. In this stage, electrochemical reactions were constantly activated in the zinc particles of coating,
and zinc/iron active area ratio increased continuously, therefore leading to a rapid decline of corrosion potential. The potential is constant during time of 350h and 1000h for the cyclic aging test and shifted the value over the cathodic protection regin. This might suggest that the presence of a protective layer and separated the carbon steel surface from the detrimental environment. In the later of cyclic time of 1000h, increment occurred for open circuit potential and could be ascribed to the corrosion of zinc particles which the corrosion products were formed on the coating surface.

3.3 Electrochemical impedance spectroscopy (EIS)

The electrochemical impedance spectroscopy analysis can provide important information about the variation of corrosion process and the protection performance of coating systems. The EIS Nyquist plots and Bode plots of carbon steel substrate coated with different graphene of zinc-rich epoxy coatings in different experiment time as shown in Fig.3. One of the most important properties of coatings is impeding the flow of current between the anode and the cathode of the metal substrate. This property is the resistance of the coating and is best characterized from EIS measurements by examining the impedance modulus |Z| at low-frequency (f=0.01Hz) $|Z|_{0.01Hz}$.

As it was shown in Fig.3, during the initial of cyclic aging experiment, the value $|Z|_{0.01Hz}$ of impedance modulus displayed high value of 10^8 Ω.cm^2 and the corresponding phase angle was close to 90°, also only one time constant can be observed in the Bode plot which indicated the good barrier characteristic of coatings and charge transfer process did not occur on the carbon steel substrate for different graphene contents of 40 wt% zinc coating[28]. This property can be attributed to the relatively low porosity of epoxy coatings and zinc particles were highly wetted by the epoxy resin. The protective property of coatings can also be attributed to the presence of graphene, and micropores and flaws inside of epoxy resin could be filled [29,30]. Additionally, graphene also acted as adhesion promoters for the steel substrate, resulted in firmly binding to the substrate with coating and the coating is not easy to fall off, so the impedance modulus of $|Z|_{0.01Hz}$ significantly increased from 10^6 Ω.cm^2 to 10^8 Ω.cm^2 for graphene modified by epoxy resin which without graphene modified epoxy resin.

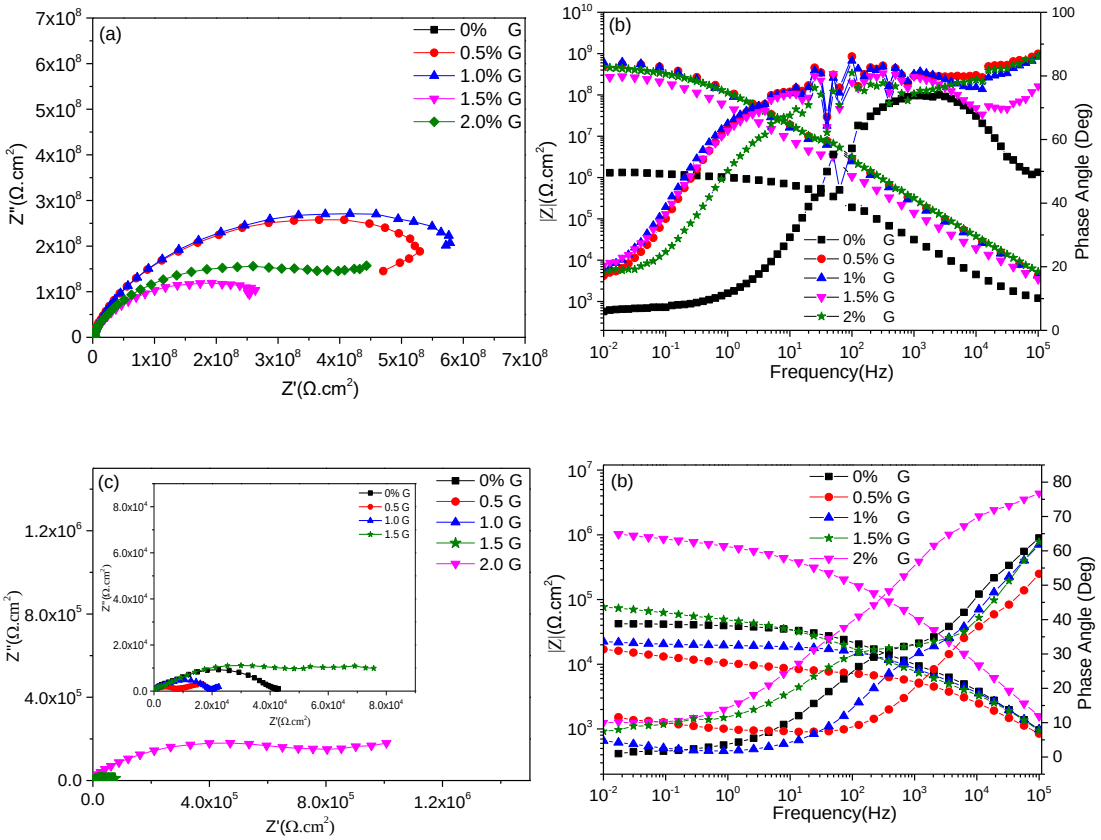

Figure 3. Electrochemical impedance spectra of steel substrate coated with different graphene contents of 40 wt% zinc-epoxy coating for different time of cyclic aging experiment (a)24h、(c) 2000h Nyquist diagram; (b)24h、(d) 2000h Bode diagram

After 2000h cyclic aging experiment, a second capacitance arc in the Nyquist plot can be found in low frequency for the graphene content of 0 wt % and 0.5 wt %. This behavior can be explained the occurrence of charge transfer resistance produced by the corrosion dissolution of zinc in the coating. However, a straight line emerges in the bode plot in fig.3 for the graphene content of 1.0 wt %, 1.5 wt %, and 2.0 wt %. This behavior is related to the increase of corrosion product for zinc particles in coating and reduced the migration rate of mass, which became the control step of corrosion reaction[31].

3.4 Electrical equivalent circuit analysis

Electrical equivalent circuits to fit impedance test data for the different contents graphene of zinc-epoxy coatings as shown in Fig.4. The equivalent circuit of model I that demostrates the water molecules absorbed by different contents graphene of zinc-epoxy coating in the initial of cyclic aging test. Rl describes the electrolyte resistance between the coating and reference electrode, and Qc and Rp represent the capacitance and percolation resistance of the epoxy coating. Rp and Qc represent the percolating resistance of coating and the capacitance characteristic of epoxy coatings. Model II indicates activation of Zn particles and Model III indicates the formation of Zn corrosion product. Rct and Qdl are shown in

model III represents the charge transfer resistance and electrical double-layer capacitance at the interface between the zinc particles and the electrolyte. *W* in model III represents the Warburg impedance and it is introduced to characterize the diffusion process of corrosive ion to steel substrate through the corrosion product layer of zinc. For all equivalent circuits, the constant phase element (Q) is used to replace capacitance because of the surface heterogeneities and dispersion effects lead to deviation from capacitive behavior.

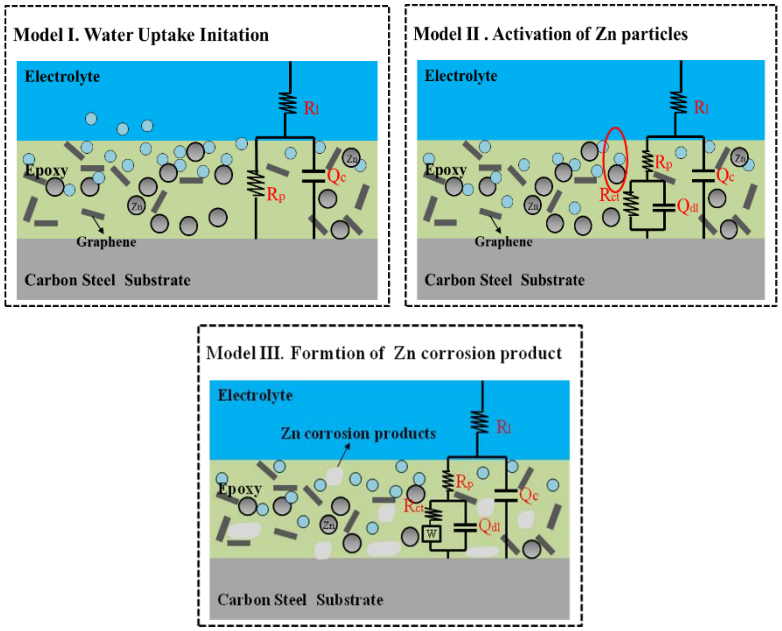

Figure 4. Electrical equivalent circuits used to fit the impedance spectra of 40 wt% zinc-rich epoxy coating with different graphene contents

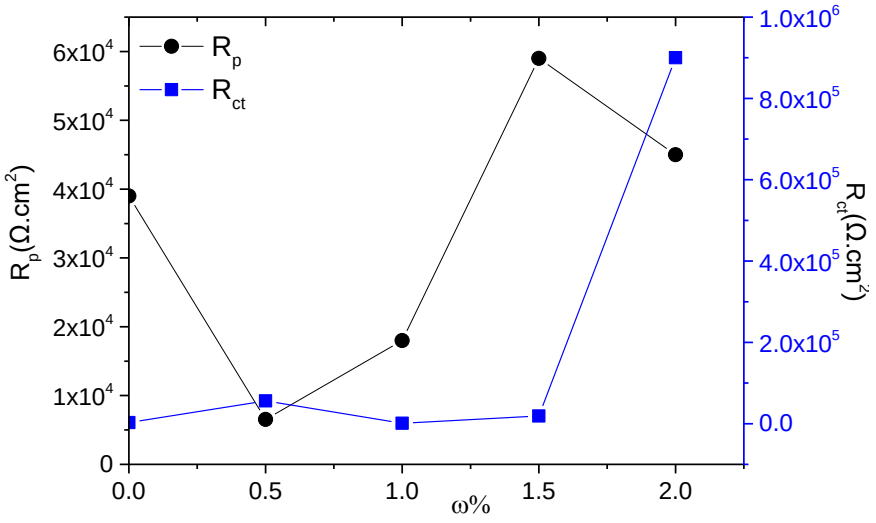

Figure 5. Variation trend of percolation resistance (R_p) and charge transfer resistance (R_{ct}) as a function of graphene contents of 40 wt% zinc-rich epoxy coating afer 2000h cyclic aging experiment

The EIS spectra of different content of graphene for zinc epoxy coating were fitted to the

equivalent circuit model. The variation trend of percolation resistance (Rp) and charge transfer resistance (Rct) of all coating samples for 2000h cyclic aging experiment are shown in fig5. As shown in fig5, the results of percolation resistance demonstrated that the epoxy coating without graphene exhibited high percolation resistance value, however, the Rp value of low content of graphene coatings less than the high content of graphene. The presence of graphene particles could increase the conductivity of coatings and it also resulted in galvanic contact with zinc particles[32].

Based on the electrical equivalent circuits of impedance spectra, in the initial stage of model I, water uptake occured inside the epoxy coating. The impedance spectra for the different content of graphene of epoxy coatings as shown in Fig. 3 and displayed a capacitive arc in the initial time of cyclic aging test. This capacitive arc may be related to the porosity of the coating for the addition of zinc fillers [37], thus the permeation of water was observed after 24 hours of cyclic aging experiment. In the diagram of fig.3(a) and (b), the Nyquist curve displayed only one capacitive arc and impedance modulus of coatings at the frequency of 0.01Hz in Bode diagram were about 1×10^8 Ω.cm2, which represented the property of barrier protection for organic coatings [38,39]. The presence of zinc oxide led to the electrically insulated the zinc particles and increased the contacted impedance. In model II, the second time constant (or capacitive arc in the Nyquist plot) can be found at low frequency after 2000h cyclic aging experiment. This may be due to the zinc oxidation and oxygen reduction reactions taking place on the zinc particles surface.This is agreement with the mechanism reported by Marchebois. [36]. Meanwhile, in the model III, a straight line emerged in the Nyquist plot of Fig.3(c) for 0.5 wt %、1.0 wt % and 2.0 wt % content of graphene. This behavior was related to mass transfer mechanism, which was the dominant process for controlling corrosion within the zinc corrosion products on the surface of carbon steel[39].

As shown in Fig.5, the electrical connection between zinc particles and graphene can be increased by adding graphene. As graphene was cathodic relative to zinc and increased the corrosion rate of sacrificial zinc particles. A large number of corrosion products were formed due to higher corrosion rate and subsequently increased the percolation resistance. Also, zinc epoxy coating modified by the graphene contained quantity of graphene particles, which was conductive of isolated zinc and electrical connection between zinc particles. The presence of a large number of active zinc particles in the anode implied a higher surface area ratio to the cathode and zinc particles can be dissolved more uniformly. The zinc-rich epoxy coating modified by graphene possessed lower charge transfer resistance. While, for the presence of a large number of graphene lamellate particles in the coating which could block the corrosive medium and therefore enhance the corrosion resistance of zinc-rich coating and lead to a increase of charge transfer resistance[18, 40-42]. Consequently, coatings exhibited better corrosion resistance in the zinc-rich epoxy coatings contained 2.0 wt % graphene.

So it was suggested that adding the appropriate amount of graphene into zinc-rich coatings can improve the percolating structure of coating and made the activation of sacrificial zinc particles more uniform. Finally, the anticorrosive and protective properties of zinc-rich coatings were improved.

3.5 SEM analysis

The SEM analysis of different content of graphene for zinc epoxy coating after 2000h cyclic

aging experiment was shown in Fig.6, the zinc particles on the surface of the coating were inordinately corroded after cyclic aging experiment. In the Fig.6a, some spherical particles on the surface of the coating without graphene was found, this could be ascribed to the bad contact of the zinc particles and led to the failure of participation in the sacrificial anodic reaction of zinc [34,35]. However, as shown in Fig.6c and Fig.6e, corrosion products connected together with increasing the content of graphene and the corrosion product became densely. The zinc-rich epoxy coating modified by 2.0 wt% of graphene which the granular zinc powders disappeared on the surface and uniformly corroded, it means that zinc powder was fully reacted and provided well cathodic protection. Graphene enhanced the electrical connection between zinc particles, so zinc powders of the coating can be completely reacted and raised the efficiency of cathodic protection. The protective effect of zinc corrosion products on the coating is also improved [33].

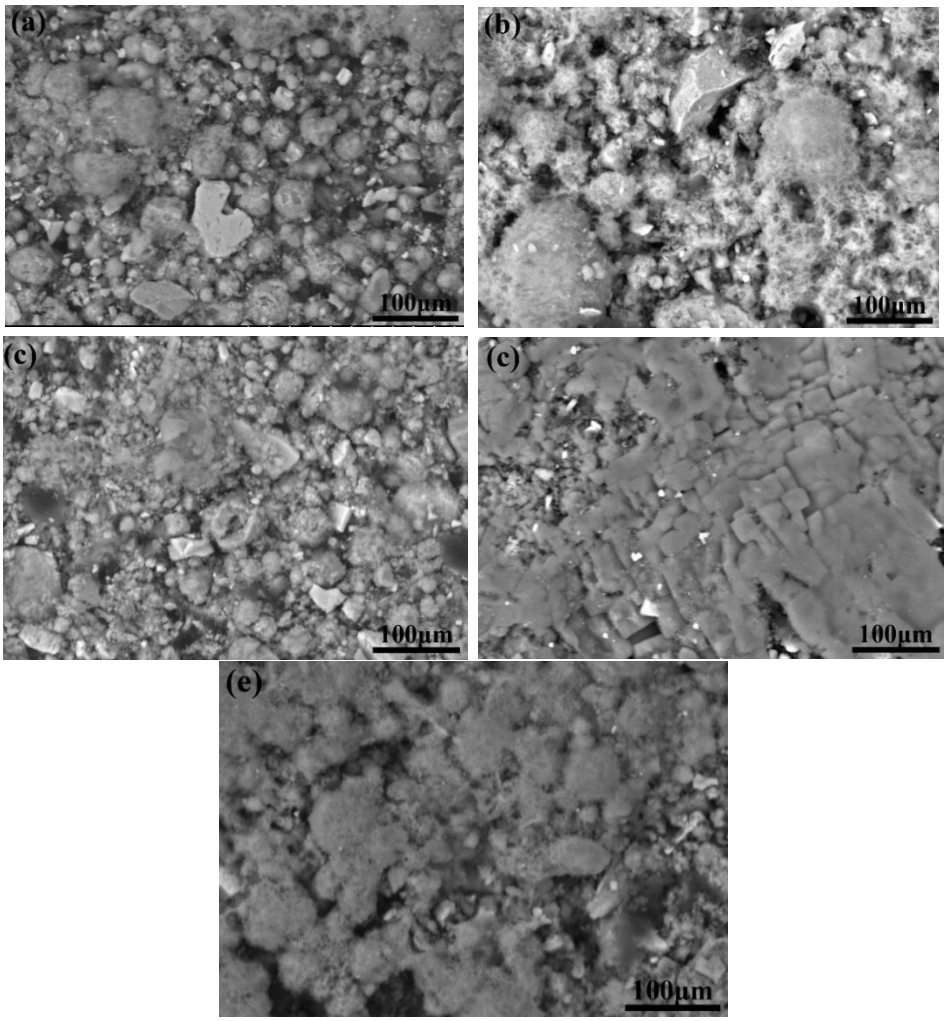

Figure 6. The SEM images of different content of graphene of the low zinc epoxy coating after 2000h cyclic aging experiment, a) 0 wt %; b) 0.5 wt %; c) 1.0 wt%; d) 1.5 wt%; e) 2.0 wt%

4. CONCLUSIONS

The anti-corrosive property of 40 wt% zinc-rich epoxy coating modified by graphene were

studied. It was found that the zinc-rich epoxy coating modified by 2.0 wt% graphene proved to be superior corrosion protection performance as compared to without graphene and with 0.5～1.5 wt% graphene particles. According to open circuit potential measurement that the more negative interface potential of 0.5 wt % and 1.5 wt % G-ZRE coatings can be attributed to the conductive effect of graphene nanoparticles, the result led to a better electrical connection between zinc particles and steel substrate. Zinc-rich epoxy coatings were modified by graphene can improve the structure of permeability of coating. Meanwhile, the addition of graphene made the activation of sacrificial zinc particles more uniform, and enhanced the anti-corrosive property of zinc-rich epoxy coatings.

ACKNOWLEDGEMENTS
This project is supported by National Key Research and Development Program (2016YFC0401205) of China.

References

1. D. M. Xie, J. M. Hu and S. P. Tong, *Acta Metall. Sin*., 40 (2004) 103.
2. R. Ding, X. Wang and J. M. Jiang, *J. Mater. Eng. Perform*., 26 (2017) 3319.
3. H.Y. Li, J.Y. Duan and D.D. Wei, *Surf. Coat. Technol.*, 235 (2013) 259.
4. K. Schaefer, A. Miszczyk, *Corros. Sci.*, 66 (2013) 380.
5. S. Pour-Ali, C. Dehghanian and A. Kosari, *Corros. Sci*., 90 (2015) 239.
6. K. Schaefer, A. Miszczyk, *Corros. Sci*., 66 (2013) 380.
7. X,G. Feng, X. Y. Liu, N. Zhuang and D. Chen, *Corros. Sci.*, 103(2016) 223.
8. B. Ramezanzadeh, S.Y. Arman and M. Mehdipour, *J. Coat. Technol. Res*., 11 (2014) 727.
9. N. Hammouda, H. Chadli, G. Guillemot and K. Belmokre, *Advanc. Chem. Eng. Sci*., 1 (2011) 51.
10. N. Tahmassebi, R. Marashi, *Tribol. Int*., 43 (2010) 685.
11. S. M. Park, M.Y. Shon, *J. Ind. Eng. Chem*., 21 (2015)1258.
12. Y. Cubides, H. Castaneda, *Corr. Sci*., 109 (2016) 145.
13. A. Gergely, Z. Pászti, J. Mihály, E. Drotár and T.Török, *Prog. Org. Coat*., 77 (2014)412.
14. A. Meroufel, S. Touzain, *Prog. Org. Coat*., 59 (2007) 197.
15. A. Gergely, É. Pfeifer, I. Bertóti, T. Török and E. Kálmán, *Corr. Sci*., 53 (2011) 3486.
16. W. B. Chen, P. Chen, H. Chen, J. Wu and W. T. Tsai, *Appl. Surf. Sci*., 187 (2002) 154.
17. K. Schaefer, A. Miszczyk, *Corr. Sci*., 66 (2013) 380.
18. B. Ramezanzadeh, M. M. Moghadam, N. Shohani and M. Mahdavian, *Chem. Eng. J*., 320 (2017) 63.
19. A. Krishnamurthy, V. Gadhamshetty, R. Mukherjee, Z.Chen, W. Ren, H-M.Cheng and N.Koratkara, *Carbon*, 56 (2013) 45.
20. W. Sun, L. D. Wang, T. T. Wu, Y. Q. Pan and G.C. Liu, *Carbon,*79 (2014) 605.
21. C. M. P. Kumar, T. V. Venkatesha and R. Shabadi, *Mater. Res. Bull*., 48 (2013) 1477.
22. T. Kuilla, S. Bhadra, D. Yao, N.H. Kim, S. Bose and J.H. Lee, *Prog. Polym. Sci*., 35 (2010) 1350.
23. M. G. Sari, M. Shamshiri and B. Ramezanzadeh, *Corr. Sci*., 129 (2017) 38.
24. K. Davies, J. Broomfield, *CRC Press*, *USA*, 2013, 259.
25. G. K. Glass, A. M. Hassanein and N. R. Buenfeld, *J. Mater. Civ. Eng*., 12 (2000) 164.
26. C. M. Abreu, M. Izquierdo, M. Keddam, X. Novoa and H. Takenouti, *Electrochim. Acta*, 41 (1996) 2405.
27. Y. H. Wu, X. Y. Zhu, W. J. Zhao, Y. J. Wang, C. T. Wang and Q. J. Xue, *J. Alloy. Compd.*, 777 (2019) 135.
28. H. Jeon, J. Park and M. Shon, *J. Ind. Eng. Chem*., 19 (2013) 849.
29. X. Chen, C. Chen, H. Xiao, F. Cheng, G. Zhang and G. Yi, *Surf. Coat. Technol*., 191 (2005) 351.
30. X. Liu, J. Xiong, Y. Lv and Y. Zuo, *Prog. Org. Coat.*, 64 (2009) 497.

31. M. Mouanga, M. Puiggali, B. Tribollet, V. Vivier, N. Pébère and O. Devos, *Electrochim. Acta*, 88 (2013) 6.
32. F. Mansfeld, *J. Appl. Electrochem*., 25 (1995) 187.
33. H. Marchebois, S. Joiret, C. Savall, J. Bernard and S. Touzain, *Surf. Coat. Technol*., 157 (2002) 151.
34. H. Hayatdavoudi, M. Rahsepar, *J. Alloy. Compd*., 727 (2017) 1148.
35. Y. Cubides, H. Castaneda, *Corr. Sci.*, 109 (2016) 145.
36. M. Mouanga, M. Puiggali, B. Tribollet, V. Vivier, N. Pébère and O. Devos, *Electrochim. Acta*, 88 (2013) 6.
37. C.M. Abreu, M. Izquierdo, M. Keddam, X.R. Nóvoa and H. Takenouti, *Electrochim. Acta*, 41 (1996) 2405.
38. F. Mansfeld, *J. Appl. Electrochem*., 25 (1995)187.
39. H. Marchebois, S. Joiret, C. Savall, J. Bernard and S. Touzain, *Surf. Coat.Technol*., 157 (2002) 151.
40. R. Ding, X. Wang, J. M. Jiang, T. J. Gui, and W. H. Li, *J. Mater. Eng. Perform*., 26 (2017) 3319.
41. Y. Cubides, H. Castaneda, *Corr. Sci.*,109 (2016) 145.
42. H. Hayatdavoudi, M. Rahsepar, *J. Alloy. Compd.*, 727 (2017) 1148.